THE JOURNAL OF BIOLOGICAL CHEMISTRY VOL. 285, NO. 37, pp. 28614–28626, September 10, 2010

The Nicotinic Acetylcholine Receptor and the Na,K-ATPase α2 Isoform Interact to Regulate Membrane Electrogenesis in Skeletal Muscle*[S]

Received for publication, June 3, 2010 Published, JBC Papers in Press, July 1, 2010, DOI 10.1074/jbc.M110.150961

Judith A. Heiny[‡], Violetta V. Kravtsova[§], Frederic Mandel[‡], Tatiana L. Radzyukevich[‡], Boubacar Benziane[¶], Alexander V. Prokofiev[§], Steen E. Pedersen[‖], Alexander V. Chibalin[¶], and Igor I. Krivoi[§1]

From the [§]Department of General Physiology, St. Petersburg State University, St. Petersburg 199034, Russia, the [‡]Department of Molecular and Cellular Physiology, University of Cincinnati, Cincinnati, Ohio 45267, the [‖]Department of Molecular Physiology and Biophysics, Baylor College of Medicine, Houston, Texas 77030, and the [¶]Department of Molecular Medicine and Surgery, Integrative Physiology, Karolinska Institutet, S-171 77 Stockholm, Sweden

The nicotinic acetylcholine receptor (nAChR) and the Na,K-ATPase functionally interact in skeletal muscle (Krivoi, I. I., Drabkina, T. M., Kravtsova, V. V., Vasiliev, A. N., Eaton, M. J., Skatchkov, S. N., and Mandel, F. (2006) *Pflugers Arch.* 452, 756–765; Krivoi, I., Vasiliev, A., Kravtsova, V., Dobretsov, M., and Mandel, F. (2003) *Ann. N.Y. Acad. Sci.* 986, 639–641). In this interaction, the specific binding of nanomolar concentrations of nicotinic agonists to the nAChR stimulates electrogenic transport by the Na,K-ATPase α2 isozyme, causing membrane hyperpolarization. This study examines the molecular nature and membrane localization of this interaction. Stimulation of Na,K-ATPase activity by the nAChR does not require ion flow through open nAChRs. It can be induced by nAChR desensitization alone, in the absence of nicotinic agonist, and saturates when the nAChR is fully desensitized. It is enhanced by non-competitive blockers of the nAChR (proadifen, QX-222), which promote non-conducting or desensitized states; and retarded by tetracaine, which stabilizes the resting nAChR conformation. The interaction operates at the neuromuscular junction as well as on extrajunctional sarcolemma. The Na,K-ATPase α2 isozyme is enriched at the postsynaptic neuromuscular junction and co-localizes with nAChRs. The nAChR and Na,K-ATPase α subunits specifically coimmunoprecipitate with each other, phospholemman, and caveolin-3. In a purified membrane preparation from *Torpedo californica* enriched in nAChRs and the Na,K-ATPase, a ouabain-induced conformational change of the Na,K-ATPase enhances a conformational transition of the nAChR to a desensitized state. These results suggest a mechanism by which the nAChR in a desensitized state with high apparent affinity for agonist interacts with the Na,K-ATPase to stimulate active transport. The interaction utilizes a membrane-delimited complex involving protein-protein interactions, either directly or through additional protein partners. This interaction is expected to enhance neuromuscular transmission and muscle excitation.

The nicotinic acetylcholine receptor (nAChR)[2] and the Na,K-ATPase are integral membrane proteins that play key roles in membrane excitation. We previously identified a regulatory mechanism, termed acetylcholine (ACh)-induced hyperpolarization, whereby the nAChR and the Na,K-ATPase functionally interact to modulate the membrane potential of rat skeletal muscle (1–4). In this interaction, the binding of nanomolar concentrations of ACh to the nAChR stimulates electrogenic transport by the Na,K-ATPase α2 isozyme, causing a membrane hyperpolarization of about −4 mV. This effect requires prolonged exposure to nanomolar concentrations of nicotinic agonist. This property distinguishes it from the more well characterized, rapid action of micromolar concentrations of ACh, which open the nAChR and produce membrane depolarization (5). This finding suggested that a non-conducting conformation of the nAChR, rather than the open state, is involved in signaling to the Na,K-ATPase. In addition, it was shown that the nAChR and Na,K-ATPase can reciprocally interact in a membrane preparation from the *Torpedo* electric organ (1), a muscle-derived tissue that is rich in muscle nAChRs and Na,K-ATPase. This finding suggested that the nAChR and Na,K-ATPase may interact as part of a membrane-associated regulatory complex.

Importantly, this regulation of Na,K-ATPase activity by the nAChR operates under the physiological conditions of normal muscle use. Its ACh concentration dependence is in the range of the residual ACh concentrations that remain in the muscle interstitial spaces for some time following nerve excitation, and to the ACh concentrations that arise at the neuromuscular junction (NMJ) from non-quantal ACh release. The later have also been shown to activate the Na,K-ATPase and hyperpolarize the end plate membrane (6, 7). Notably, this hyperpolariza-

* This work was supported, in whole or in part, by National Institutes of Health Grant HL6606, Russian Foundation for Basic Research 10-04-00970a, the Physiology Research Fund of the University of Cincinnati, the Swedish Research Council, Novo-Nordisk Foundation, Hedlunds Foundation, and Commission of the European Communities Grants LSHM-CT-2004-512013 EUGENEHEART and LSHM-CT-2004-005272 EXGENESIS.

We dedicate this article to the memory of Frederic Mandel, who tragically passed away in 2009. Dr. Mandel made many seminal contributions to our understanding of the Na-K-ATPase in his more than 30 years in the field, and proposed the research that led to these findings.

[S] The on-line version of this article (available at http://www.jbc.org) contains supplemental Fig. S1.

[1] To whom correspondence should be addressed: Department of General Physiology, St. Petersburg State University, 7/9 University emb., St. Petersburg 199034, Russia. Tel.: 7-812-3289741; Fax: 7-812-3289703; E-mail: iikrivoi@gmail.com.

[2] The abbreviations used are: nAChR, nicotinic acetylcholine receptor; ACh, acetylcholine; NMG-Cl, *N*-methyl-D-glucamine chloride; NMJ, neuromuscular junction; BTX, bungarotoxin.

tion is generated in the voltage range of muscle sodium channel slow inactivation, where the availability of sodium channels increases ~3-fold per each 6 mV change in membrane potential (8, 9). Thus, the physiological consequence of a small hyperpolarization near the resting potential is expected to be more effective neuromuscular transmission and muscle excitation.

This study examines the molecular mechanisms and membrane localization of the interaction between the nAChRs and the Na,K-ATPase. We tested the hypothesis that a non-conducting, desensitized conformation of the nAChR mediates signaling to the Na,K-ATPase. We examined whether Na^+ entry through the nAChR in a conducting state is required for the effect. We also used non-competitive antagonists of the nAChR, which shift the equilibrium distribution of nAChRs between resting and desensitized conformations in opposite directions. In addition, we tested the hypothesis that the regulatory interaction between the nAChR and Na,K-ATPase occurs in a membrane-delimited complex and involves protein-protein interactions. To test this, we examined whether the muscle nAChR and the Na,K-ATPase co-immunoprecipitate, and we used confocal microscopy with cytochemistry to determine their membrane localization. Finally, we used a highly purified membrane preparation of nAChRs and the Na,K-ATPase from NMJs of the *Torpedo* electric organ to further identify which conformational state of the nAChR interacts with the Na,K-ATPase. Our results suggest that the nAChR in a desensitized state and the Na,K-ATPase $\alpha 2$ isoform interact as a regulatory complex whose function is to modulate membrane electrogenesis.

EXPERIMENTAL PROCEDURES

Materials—ACh, ouabain, proadifen, QX-222, tetracaine, and nicotine ((−)nicotine hydrogen tartrate), and diisopropyl fluorophosphates were obtained from Sigma. α-Bungarotoxin was from Molecular Probes (Eugene, OR) and [^{3}H]ouabain was obtained from Amersham Biosciences. All other chemicals were of analytical grade (Sigma).

Animals—Membrane potential experiments and biochemical assays were performed using freshly isolated diaphragm muscles from adult male Wistar rats (180–200 g). The rats were anesthetized (ether) and euthanized by cervical dislocation prior to tissue removal. Two hemidiaphragms were dissected from each rat. A strip from the left hemidiaphragm was used immediately for electrophysiological experiments; the remaining diaphragm tissue was quickly frozen in liquid nitrogen for biochemical assays. Confocal imaging was performed on extensor digitorum longus muscles isolated from WT mice or $\alpha 2^{R/R}$ transgenic mice from a colony maintained at the University of Cincinnati (10). The $\alpha 2^{R/R}$ mice express a Na,K-ATPase $\alpha 2$ subunit that is resistant to the binding of ouabain. Tissue removal was performed using anesthesia (2.5% Avertin, 17 ml/kg) and the animals were euthanized after the experiment. All procedures on mice were approved by the University of Cincinnati Institutional Animal Care and Use Committee. *Torpedo californica* tissue was purchased frozen (Aquatic Research Consultants, San Pedro, CA).

Membrane Potential Recording—A 10–15-mm wide diaphragm strip with the nerve stump was placed in a 2-ml Plexiglas chamber and continuously perfused with a physiological solution containing (mM): NaCl, 137; KCl, 5; $CaCl_2$, 2; $MgCl_2$, 2; $NaHCO_3$, 24; NaH_2PO_4, 1; glucose, 11; pH 7.4. The solution was continuously bubbled with 95% O_2 and 5% CO_2 and maintained at 28 °C. The muscle was allowed to equilibrate for 1 h before the start of recording. In some experiments, extracellular NaCl was replaced with *N*-methyl-D-glucamine chloride (NMG-Cl). NMG^+ is an impermeant cation commonly used to prevent Na^+ entry (11). Resting potentials were recorded intracellularly using standard microelectrode techniques. Glass microelectrodes were filled with 3 M KCl and had resistances <10 megaOhm. The resting potential was amplified and digitized (44.1 kHz, 12-bit) using a PC computer running custom software, which automated and standardized data collection. A digital trigger to the acquisition system was sent immediately before impalement to record and correct the electrode-to-solution potential (zero balance) and after impalement to record the resting potential. Using this procedure, the resting potential was recorded from each fiber within 1–2 s of impalement, and an average of 10 s elapsed between recordings from different fibers. This protocol is optimized for accurate measurement of small differences in membrane potential and is more appropriate for this study than continuous recording, because temporal drifts of even a few millivolts can distort the measurement. Multiple measurements of short duration are commonly used for measuring the electrogenic activity of the Na,K-ATPase in skeletal muscle (7, 12).

Recordings were made in extrajunctional membrane regions within ~1–2 mm from visually identified terminal branches of the nerve, or directly at the nerve terminal (junctional membrane). Resting potentials were recorded from 25 to 35 different fibers within each muscle. The total recording time for this determination, including solution change and time to impale the fibers, was 5–10 min. The entire protocol was repeated at different time intervals and in muscles from different animals to obtain the average resting potential for that time interval and condition. Thus, the resting potential reported at each nominal time point represents the mean ± S.E. of measurements from a total of 100–170 fibers obtained from 3–6 muscles in the indicated condition.

Membrane input resistance was measured using a single-electrode bridge balance protocol as described (13). The input resistance depends on the membrane resistance and the resistance of fluids inside and outside the cell. Because the resistance of the intracellular and extracellular fluids were constant in our conditions, a change in input resistance directly reflects a change in membrane resistance.

Measurement of Na,K-ATPase Electrogenic Activity in Intact Skeletal Muscle—The electrogenic activity of the Na,K-ATPase in intact skeletal muscle was measured as the ouabain-inhibitable component of the resting membrane potential, as described previously (1, 2, 4) (see also Fig. 6). Active transport by the Na,K-ATPase generates a negative membrane potential (E_{pump}) due to the net outward transfer of one positive charge per transport cycle. E_{pump} adds directly to the Nernst potential (E_{Nernst}) arising from the ion concentration differences and brings the resting membrane potential to a more negative value than expected from the ion gradients alone (resting membrane

potential = E_{Nernst} + E_{pump}) (14). This ouabain-inhibitable component of the resting membrane potential directly reports electrogenic transport by the Na,K-ATPase. The electrogenic contribution to the resting potential is large in skeletal muscle, reflecting the high Na,K-ATPase content of this tissue, and can be used to follow changes in Na,K-ATPase activity under different conditions.

Measurement of Muscle Intracellular Na^+—Intact soleus muscles were dissected out and split longitudinally into two muscle strips. The muscles were mounted at resting length in a Krebs-Ringer bicarbonate buffer (pH 7.4; 30 °C), which was bubbled continuously with 95% O_2 and 5% CO_2. Muscles were incubated either in the absence or presence of 5 μM proadifen for 30 min, followed by 100 nM nicotine for 1 h. Then, the intracellular Na^+ content was measured using a published procedure (15). In brief, the muscles were transferred to ice-cold Na^+-free Tris-sucrose buffer and underwent four 15-min washouts to remove extracellular Na^+. Following washout, muscles were blotted, the tendons were cut off, muscle wet weight was determined, and the muscles were soaked overnight in 0.3 ml of trichloroacetic acid (TCA) to completely extract ions from the tissue. The Na^+ content in the TCA extract was measured by flame photometry (FLM3, Radiometer) with lithium as the internal standard. Values were expressed as micromoles of Na^+/g wet weight.

Co-immunoprecipitation—Muscles were pulverized in liquid nitrogen and solubilized in lysis buffer (137 mM NaCl, 2.7 mM KCl, 1 mM $MgCl_2$, 20 mM Tris, pH 8.0, 1% Triton X-100, 10% (v/v) glycerol, 10 mM NaF, 0.5 mM Na_3VO_4, 5 μg/ml leupeptin, 0.2 mM phenylmethylsulfonyl fluoride, 5 μg/ml aprotinin, and 1 μM microcystin) for 1 h at 4 °C with continuous rotation. The resulting lysate was centrifuged for 10 min at 3,000 × *g* to pellet insoluble material. The supernatant was collected and kept on ice. The pellet was re-suspended in lysis buffer and centrifuged again for 10 min at 3,000 × *g*. The supernatants contained >99% of total Na,K-ATPase protein and were combined. Less than 0.5% of the Na,K-ATPase protein present in the initial lysate was detected in the final pellet by Western blot. Protein concentration was determined using the BCA™ protein assay kit (Pierce). Immunoprecipitation was carried out using rabbit polyclonal antibody against the Na,K-ATPase α1 (Cell Signaling, number 3010) and rabbit polyclonal antibody to the Na,K-ATPase α2 subunit (kindly provided by Dr. T. Pressley, Texas Tech University Health Sciences Center, Lubbock, TX) specific monoclonal antibodies against the Na,K-ATPase α1 (clone 6H, kindly provided by Dr. M. Caplan, Yale University, New Haven, CT) and α2 subunits (clone McB2, kindly provided by Dr. K. Sweadner, Massachusetts Central Hospital, Boston, MA) and the nAChR α_1-subunit (Abcam ab11149), followed by affinity purification using Protein G and Protein A magnetic Dynabeads® (Invitrogen). After incubation with beads for 1 h at room temperature, the immunocomplex was washed twice in lysis buffer and three times in PBS. The protein samples were heated for 20 min at 56 °C in loading buffer, run on gradient 6–20% SDS-polyacrylamide gels, and probed with the primary antibody and horseradish peroxidase-conjugated secondary antibody (goat anti-rabbit and anti-mouse IgG; Bio-Rad). The primary antibodies used for Western blot were: a specific monoclonal antibody against the Na,K-ATPase α1 (clone 6H), an anti-Na,K-ATPase α2subunit (clone McB2), an anti-caveolin-3 antibody (Abcam ab2912), anti-phospholemman (FXYD1) antibody (ProteinTech Group Inc., 13721-1-AP), anti-SERCA2 antibody (Abcam ab2861), and anti-phospholamban antibody (Cyclacel, UK; 010-14). Protein bands were visualized by enhanced chemiluminescence (Amersham Biosciences) and quantified by densitometry.

Confocal Microscopy and Co-localization—For imaging unfixed muscle, a freshly isolated mouse extensor digitorum longus muscle was superfused with physiological saline containing 0.6 μM rhodamine-conjugated bungarotoxin and 0.5–1 μM BODIPY-conjugated ouabain (Invitrogen). Superficial regions of the muscle were imaged with a ×40, 1.2 NA objective using a Zeiss 510 Meta laser confocal system configured for concurrent viewing of rhodamine and BODIPY fluorescence. Rhodamine spectra were: λ_{ex} 488 nm at 5%, λ_{em} 565–615 nm; BODIPY spectra were: λ_{ex} 488 nm, λ_{em} 500–545 nm. Identical imaging settings were used on both channels. For imaging fixed tissue, a mouse EDL muscle was coated with OCT (Tissue Tek) and frozen in liquid nitrogen. Transverse sections were cut (8 μm; Leica cryostat), placed on glass slides, fixed in 100% acetone at −25 °C for 5 min, and transferred to PBS (pH 7.2). Antibody retrieval was performed using 10 mM sodium citrate with 0.5% Tween 20 (pH 8) at 65 °C for 20 min, and washed in PBS. The sections were blocked using 10% normal goat serum in PBS, incubated in primary antibody, washed in PBS, incubated in secondary antibody, and washed in PBS. The primary antibody was a Na,K-ATPase α2-specific polyclonal antibody, affinity purified from antisera generated using the synthetic HERED peptide (16, 17) and used at 1:50 dilution in PBS with 10% serum. The secondary antibody was a F(ab′) fragment of goat anti-rabbit IgG (H + L) conjugated to Alexa Fluor 594 (Invitrogen) and used at 1:200 dilution in PBS with 10% normal goat serum. Sections were incubated in secondary antibody at room temperature and washed in PBS. After labeling with the Na,K-ATPase antibody, the sections were incubated with 5 μM Alexa Fluor 555-conjugated α-bungarotoxin (Invitrogen), mounted on slides (Fluoromount-G, Southern Biotech), and washed. Sections were imaged using a Zeiss 510 Meta laser confocal system equipped with a 100×, 1.45 NA objective and configured for multitrack acquisition of Alexa Fluor 594 (λ_{ex} 543 nm; λ_{em} 670–703 nm) and Alexa Fluor 555 (λ_{ex} 543 nm, λ_{em} 550–600 nm) fluorescence. Identical settings were used on both channels. Images were analyzed using Zeiss LSM software. Because histological techniques are subject to intersample variability, images are shown only if seen in at least three different samples processed independently.

Rapid Stopped-flow Fluorescence Spectroscopy—Purified membranes enriched in the nAChR and Na,K-ATPase were isolated from *T. californica* electric organ by differential sucrose ultracentrifugation (18). This preparation contains large quantities of both muscle type nAChRs and the Na,K-ATPase (18, 19). The membrane preparation typically contained 1–1.6 nmol of nAChR binding sites/mg of protein, determined by either [^{3}H]ACh binding or [^{125}I]α-bungarotoxin binding; and 0.1–0.25 nmol of Na,K-ATPase binding sites/mg of protein as determined by [^{3}H]ouabain binding. Membranes

were stored in 37% sucrose, 0.2% NaN_3 at −80 °C under argon. Immediately prior to use, the membranes were treated with diisopropyl fluorophosphate to inactivate acetylcholinesterase typically present in this preparation.

Binding of the fluorescent cholinergic ligand 5-dimethylaminonaphthalene 1-sulfonyl C6-choline (dansyl C6 choline, D6C6; (20)) to the nAChR was monitored by changes in fluorescence intensity at 557 nm. DC6C was excited using energy transfer from a tryptophan near the ACh binding sites (21, 22), as described previously (1). The assays were conducted in *Torpedo* physiological saline buffer, HTPS (250 mM NaCl, 5 mM KCl, 3 mM $CaCl_2$, 2 mM $MgCl_2$, and 20 mM Hepes, pH 7.0). The rapid kinetic experiments were carried out with a stopped-flow instrument (KinTek Corporation, Austin, TX, model SF-2001). The membranes were incubated with 0 (control), 10, or 20 nM ouabain for 1 h and then rapidly mixed with 1 μM DC6C. The concentration of nAChR used was typically 100 or 200 nM ACh binding sites (~0.06–0.20 mg/ml). The fluorescence intensity upon agonist binding was monitored from ~1 ms to 15 s. Ten to 20 individual mixing traces were averaged to obtain a single averaged curve.

Data Analysis—Values are given as the mean ± S.E. The statistical significance of differences between means was evaluated using a Student's *t* test (ORIGIN 6.1. software).

RESULTS

The Functional Interaction Between the nAChR and the Na,K-ATPase in Skeletal Muscle Does Not Require Na^+ Entry Through Open nAChRs—We previously showed that 100 nM ACh or nicotine, acting on the nAChR, hyperpolarizes the nonjunctional membrane of skeletal muscle by approximately −4 mV. Nanomolar concentrations of ouabain or marinobufagenin prevent this hyperpolarization, indicating that it results specifically from increased electrogenic transport by the α2 Na,K-ATPase (1–4).

The ability of nanomolar concentrations of nicotinic agonists to *hyper*polarize the resting potential contrasts with the well known ability of micromolar concentrations of ACh to open the nAChR, producing membrane *de*polarization (5). This suggested that the mechanism by which the nAChR stimulates the Na,K-ATPase does not require current flow through open nAChRs. Nevertheless, a small but finite number of nAChRs are opened by nanomolar ACh (23). Therefore, a possible mechanism of the ACh-induced hyperpolarization could be substrate stimulation of the Na,K-ATPase by Na^+ entering through open nAChRs. To test this possibility, we examined whether the hyperpolarization remains when extracellular NaCl is replaced with NMG-Cl. NMG^+ alone (Fig. 1, *open circles*) does not alter the membrane potential. However, addition of 100 nM nicotine (*closed circles*) hyperpolarizes the membrane by −4.5 mV ($p < 0.01$). The magnitude and time course of this effect are similar to that consistently seen in control, Na^+-containing solutions (1). This result suggests that Na^+ entry through the nAChR is not required for its functional interaction with the Na,K-ATPase.

This interpretation was further tested by comparing the changes in membrane permeability and intracellular [Na^+] that occur when nanomolar nicotine is applied to nAChRs stabilized in either the resting or the desensitized conformation. Small increases in membrane permeability and intracellular [Na^+] are expected if nicotine initially opens a small number of nAChRs before they spontaneously desensitize. Both of these effects occur in rat skeletal muscle (Fig. 2). When 100 nM nicotine is applied under control conditions, in which nAChRs are initially in the resting state, nicotine induces a 21% decrease ($p < 0.01$) in the membrane input resistance (Fig. 2*A*), indicating increased membrane permeability. In parallel, 100 nM nicotine causes a small but significant ($p < 0.01$) increase in intracellular [Na^+] (Fig. 2*B*). These changes are prevented by preincubating the muscle in 5 μM proadifen. Proadifen is a noncompetitive blocker of the nAChR, which shifts the distribution of nAChRs from resting to non-conducting, desensitized states (23–25). Proadifen alone has no effect on intracellular [Na^+]. This result is consistent with our previous findings that the sustained hyperpolarization induced by nanomolar ACh or nicotine is sometimes preceded by a small depolarization (1, 4); and that 5 μM proadifen prevents this depolarization without effect on the sustained hyperpolarization (4).

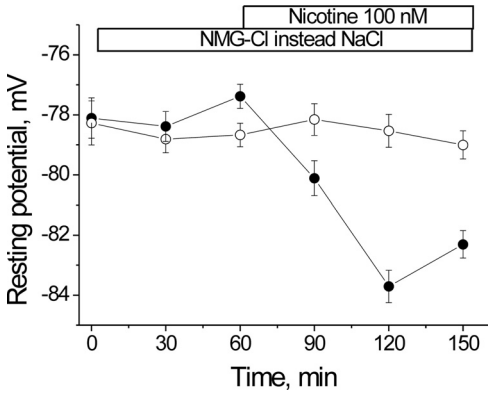

FIGURE 1. **The nicotine-induced membrane hyperpolarization does not require Na^+ entry.** Membrane potentials were measured from extrajunctional membrane regions of isolated rat diaphragm perfused with a solution in which extracellular NaCl was replaced with NMG-Cl, in the absence (*open circles*) and presence (*filled circles*) of 100 nM nicotine. *Horizontal bars* indicate the periods when NMG-Cl and/or nicotine were present.

Collectively, these results show that nicotinic agonists at nanomolar concentrations have two distinct actions on the membrane potential, a depolarizing action associated with opening a small fraction of nAChRs, and a hyperpolarizing action that requires Na,K-ATPase activity but not Na^+ entry. The hyperpolarization occurs by a mechanism that is distinct from, and does not require, nAChR opening.

A Desensitized State of the nAChR Mediates Its Interaction with the Na,K-ATPase—The nAChR can assume resting (micromolar agonist affinity), open, or desensitized conformations (non-conducting states with nanomolar apparent affinity for agonist) (26–29). High concentrations of ACh promote channel opening followed by spontaneous transitions to the desensitized state. Desensitized states can also occur without channel opening and are favored after prolonged exposure to low concentrations of agonist. The results in Figs. 1 and 2 together with our previous results suggest that a non-conducting state of the nAChR with apparent high affinity for agonist, possibly a desensitized state, mediates the stimulation of Na,K-ATPase activity (1, 3, 4). If this is the case, it should be possible

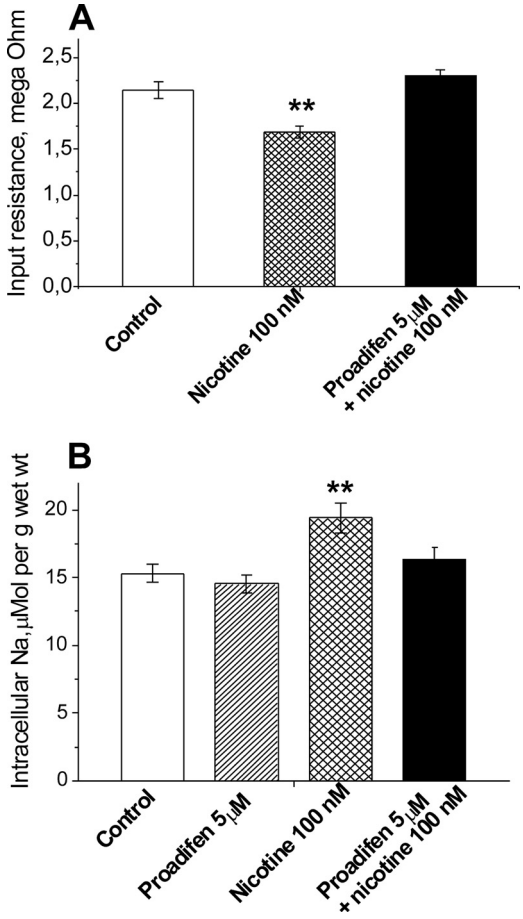

FIGURE 2. **Nanomolar concentrations of nicotine produce small increases in membrane permeability and intracellular [Na^+].** *A*, effect of 100 nM nicotine on the input resistance of diaphragm muscle fibers in the absence and presence of 5 μM proadifen. Input resistance was measured as described under "Experimental Procedures" at extrajunctional regions of muscles incubated in control solution, during 30–60 min after addition of nicotine, or during 30–60 min after addition of nicotine plus proadifen. Proadifen was added for 30 min prior to the addition of nicotine. ** $p < 0.01$ compared with control. Decreased membrane input resistance indicates increased membrane permeability. $n = 130$–196 fibers in each condition. *B*, effect of 100 nM nicotine on the intracellular [Na^+] of soleus muscle fibers preincubated in control solution, in 5 μM proadifen, 100 nM nicotine alone, and 100 nM nicotine plus 5 μM proadifen. Intracellular [Na^+] (micromoles per g wet weight) was measured as described under "Experimental Procedures." Muscles were incubated in each solution for 30 min followed by 60 min in 100 nM nicotine, or, in control followed by 30 min in proadifen prior to the addition of nicotine. $n = 8$ muscles in each condition; **, $p < 0.01$ compared with control.

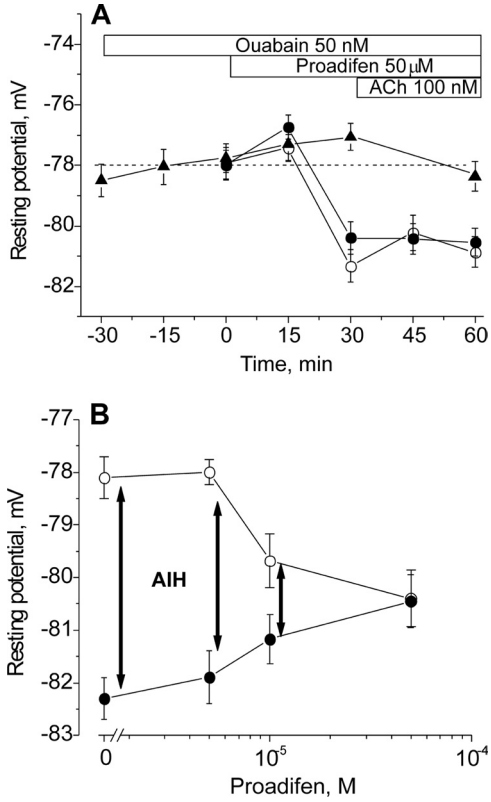

FIGURE 3. **Changes in the resting membrane potential of rat diaphragm muscle induced by proadifen.** *A*, changes in membrane potential produced by 50 μM proadifen alone (*open circles*), 50 μM proadifen followed by 100 nM ACh (*closed circles*), and 50 μM proadifen in the presence of 50 nM ouabain (*triangles*). Ouabain incubation was started 30 min prior to adding the test solutions. *Horizontal bars* indicate the periods when proadifen, ACh, or ouabain was present. *B*, resting membrane potentials recorded in the presence of different concentrations of proadifen (30 min preincubation, *open circles*), and 15 min after the subsequent addition of 100 nM ACh (*filled circles*). ACh-induced hyperpolarization (*AIH*) (*vertical arrows*) was computed as the difference between the resting potential measured before and after 15 min in ACh. Membrane potentials were recorded from extrajunctional membrane regions.

to induce membrane hyperpolarization directly from the desensitized nAChR, without agonist binding. Therefore, we examined whether proadifen at higher concentrations is able to induce membrane hyperpolarization in the absence of nicotinic agonists. As shown in Fig. 3*A*, 50 μM proadifen induces a hyperpolarization of approximately -3 mV ($p < 0.01$) in rat skeletal muscle. This hyperpolarization is prevented by preincubation with 50 nM ouabain, indicating that it results from stimulated electrogenic transport by the Na,K-ATPase $\alpha 2$ isozyme. (The rodent $\alpha 1$ isozyme is >100-fold less sensitive to ouabain binding.) On the other hand, when 100 nM ACh is applied to nAChRs already desensitized by proadifen, it does not produce additional hyperpolarization. These results indicate that the functional interaction between nAChRs and the Na,K-ATPase is maximal when the nAChRs are maximally desensitized.

This conclusion is further supported by the measurements in Fig. 3*B*, which show the effect of preincubating the muscle with increasing concentrations of proadifen *prior* to adding 100 nM ACh. Proadifen alone at low concentrations (up to 5 μM) does not induce hyperpolarization; in this condition, the subsequent addition of 100 nM ACh is able to hyperpolarize the membrane by -4 mV. However, preincubation with increasing concentrations of proadifen (10–50 μM) produces membrane hyperpolarization in the absence of ACh. In parallel, the ability of ACh to cause hyperpolarization is diminished. This result indicates that the interaction between the nAChR and the Na,K-ATPase occurs when the nAChR is in a desensitized state, irrespective of the pathway by which the nAChR becomes desensitized. Either prolonged exposure to nanomolar concentrations of nicotinic agonists, or proadifen alone at 10–50 μM, produce nAChR desensitization and membrane hyperpolarization. This result further supports our proposal that nAChR in a desensitized state is able to signal to the Na,K-ATPase to stimulate its transport activity.

Proadifen, in addition to promoting nAChR desensitization, also blocks voltage-dependent sodium channels. Therefore, it is

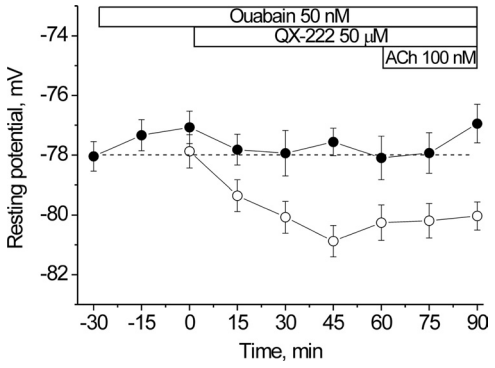

FIGURE 4. **Changes in the resting membrane potential of rat diaphragm muscle induced by QX-222.** Changes in membrane potential produced by 50 μM QX-222 alone followed by the addition of 100 nM ACh (*open circles*), and 50 μM QX-222 in the presence of 50 nM ouabain (*closed circles*; ouabain incubation was started 30 min prior to the test solutions). *Horizontal bars* indicate the periods when QX-222, ACh, or ouabain was present. Membrane potentials were recorded from extrajunctional membrane regions.

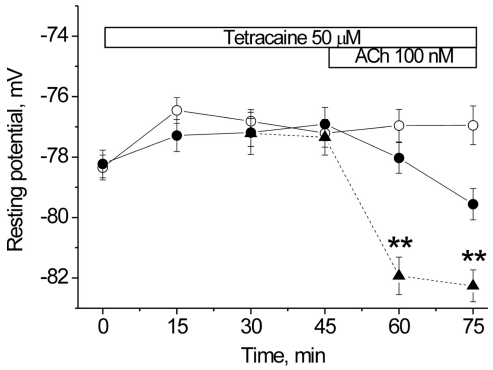

FIGURE 5. **Changes in the resting membrane potential of rat diaphragm muscle induced by tetracaine.** Changes in membrane potential produced by 50 μM tetracaine alone (*open circles*), by 50 μM tetracaine followed by the addition of 100 nM ACh (*closed circles*). *Triangles* show the effect of 100 nM ACh in normal physiological solution, at 60 and 75 min. These points superimpose on previous measurements of the effect of 100 nM ACh in normal physiological saline at long times (*dashed line*, from Ref. 1). *Horizontal bars* indicate the periods when tetracaine or ACh was present. Membrane potentials were recorded from extrajunctional membrane regions. **, $p < 0.01$ compared with ACh-induced hyperpolarization in normal physiological solution.

possible that the hyperpolarization produced by proadifen could result from block of a basal Na^+ current through one of these channels. To further exclude an ionic mechanism, we tested the actions of QX-222 and tetracaine. QX-222 and tetracaine, like proadifen, are local anesthetics and non-competitive blockers of the nAChR. However, they produce block by promoting different conformational states of the nAChR. QX-222 blocks the open channel (30), whereas tetracaine lowers the affinity for ACh and shifts the equilibrium distribution to resting conformations (31). As shown in Fig. 4, 50 μM QX-222 alone induces a hyperpolarization of approximately -3 mV ($p < 0.01$) and the hyperpolarization is not increased further by application of 100 nM ACh. Moreover, the hyperpolarization induced by QX-222 is prevented by preincubation with 50 nM ouabain (30 min), confirming that it arises from stimulated electrogenic transport by the Na,K-ATPase α2 isozyme.

In contrast, 50 μM tetracaine alone does not cause hyperpolarization (Fig. 5). Were a basal Na^+ current present, tetracaine should have blocked it, causing hyperpolarization. However, when ACh is applied after preincubation with tetracaine, the ACh-induced hyperpolarization is significantly retarded. This effect is directly expected from the ability of tetracaine to stabilize the resting nAChR conformation. It is also consistent with our previous demonstration that pretreatment of skeletal muscle with α-bungarotoxin (5 nM), which locks nAChRs in a non-conducting conformation, prevents the ACh-induced hyperpolarization (1).

Collectively, the results in Figs. 3–5 demonstrate that the nAChR in a non-conducting, desensitized state can stimulate electrogenic transport by the Na,K-ATPase and, thereby, membrane hyperpolarization. The actions of each of these compounds on the ACh-induced hyperpolarization vary as expected from their well characterized ability to shift the equilibrium distribution of nAChRs between resting and desensitized conformations.

The Functional Interaction between the nAChR and the Na,K-ATPase α2 Isozyme Operates on Both Junctional and Extrajunctional Membrane Regions—The membrane potentials shown in Figs. 1–5 as well as our previous measurements (1–4) were recorded from extrajunctional regions of the muscle membrane, within 1–2 mm of the NMJ. Because this distance is 2–3 times the length constant of diaphragm muscle, it indicates that the measured hyperpolarization must originate from extrajunctional nAChRs and Na,K-ATPase. Although less dense than at the NMJ, nAChRs are present on extrajunctional sarcolemma at about 40 per μm^2 (32).

Other studies have shown that the low levels of ACh resulting from non-quantal release (~50 nM) at the NMJ hyperpolarize the junctional membrane by approximately -3 mV by a mechanism that involves stimulation of the Na,K-ATPase (6, 7). This local hyperpolarization keeps the junctional membrane at a slightly more negative potential than extrajunctional regions. The similarity of the ability of both exogenous and endogenous cholinergic agonists to hyperpolarize the membrane potential suggested that both phenomena may arise from a common mechanism, *i.e.* stimulation of the Na,K-ATPase by the nAChR. To investigate this, we measured the contributions of the α1 and α2 Na,K-ATPase isozymes to the membrane potential at junctional and extrajunctional membrane regions. The electrogenic contributions of the α1 and α2 isozymes to the membrane potential were separated as shown in Fig. 6 based on their different affinities for ouabain (33). In rat diaphragm muscle, 1 μM ouabain inhibits the α2 isoform without effect on the α1 isoform; whereas 500 μM ouabain completely inhibits both isoforms (2).

As shown, the sequential addition of 1 and 500 μM ouabain depolarizes the membrane stepwise as the α2 and α1 isozymes, respectively, are inhibited (Fig. 6). The resting membrane potential of the junctional membrane (*open circles*) is initially 3.5 ± 0.6 mV more negative than that of the extrajunctional membrane on the same muscle (-81.5 ± 0.4 mV, 154 fibers compared with -78.0 ± 0.4 mV, 184 fibers; $p < 0.01$), consistent with previous reports (6, 7). The addition of 1 μM ouabain depolarizes both regions to approximately -73 mV. This indicates that surplus hyperpolarization at the junctional membrane is generated by the same mechanism as that of non-junctional regions, *i.e.* electrogenic transport by the α2 Na,K-

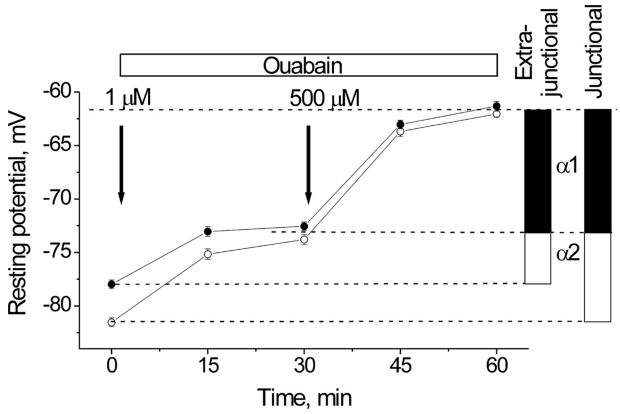

FIGURE 6. **Contributions to the resting potential from electrogenic transport by the α1 and α2 Na,K-ATPase isozymes in junctional (*open circles*) and extrajunctional (*closed circles*) membrane regions of the same diaphragm muscle fibers.** *Arrows* indicate when ouabain (1 or 500 μM) was added. *Vertical bars* indicate the electrogenic potentials (mV) contributed by the α1 (*black*) or α2 (*white*) Na,K-ATPase isozymes, computed as the difference in resting potential measured before and after blockade of the Na,K-ATPase isozymes by 1 μM ouabain (α2) or 500 μM ouabain (α1). The depolarization caused by inhibition of each isozyme becomes stable after ~30 min.

ATPase. Surplus hyperpolarization at the junctional membrane also remains when extracellular NaCl is replaced with NMG-Cl (this study),[3] consistent with its originating from an electrogenic transport rather than an ionic mechanism. The subsequent addition of 500 μM ouabain inhibits all Na,K-ATPase activity and brings the resting potential of both regions to approximately −62 mV. Thus, the basal electrogenic activity of the α1 Na,K-ATPase isozyme contributes equally at junctional and extrajunctional regions (−11.7 ± 0.6 and −11.2 ± 0.6 mV). Whereas, the electrogenic activity of the α2 isozyme is greater near the NMJ where nAChRs are concentrated and where basal, nanomolar levels of ACh are present from non-quantal release. These results show that the Na,K-ATPase α2 isozyme can be stimulated by the nAChR on both junctional and extrajunctional membrane regions, and that the amplitude of the resulting hyperpolarization is greater in regions of high nAChR density and basal ACh levels.

The nAChR and the Na,K-ATPase α2 Isoform Co-localize at the Muscle End Plate—In innervated, adult skeletal muscle, the nAChR is expressed predominantly at the postsynaptic NMJ. The Na,K-ATPase α1 and α2 subunits are also detected at the postsynaptic NMJ but their possible co-localization with the nAChR is not known. We investigated this question by imaging the NMJ of intact skeletal muscles (Fig. 7) dual labeled with fluorescent-labeled specific ligands of the Na,K-ATPase (BODIPY-conjugated ouabain, 1 μM) and the nAChR (rhodamine-conjugated bungarotoxin); and also by imaging the end-plate regions of transverse, fixed sections of skeletal muscle (Fig. 8) dual labeled with BTX and an isoform-specific antibody of the α2 Na,K-ATPase.

In *en face* views of intact skeletal muscle, the fluorescent ouabain signal overlaps with the bungarotoxin signal at the muscle end plates (Fig. 7, *A–C*). Ouabain at 1 μM is expected to label the α2 Na,K-ATPase, the only high affinity isoform present at the postsynaptic NMJ of rodents (34). This was confirmed by imaging the end plates of transgenic mice in which the α2 isoform is resistant to the binding of ouabain (10). The ouabain signal is completely absent from the α2-ouabain-resistant mice (Fig. 7, *D*, *E*), confirming that 1 μM BODIPY ouabain labels the α2 isoform, and not the α1 isoform. The distribution of α2 Na,K-ATPase is expected to be broader than that of BTX because the α2 Na,K-ATPase isozyme is also expressed in sarcolemma and transverse tubules. Consistent with this expectation, the fluorescent ouabain signal is also detected on non-junctional sarcolemma and in the transverse tubules (Fig. 7*F*). As an additional positive control, the ouabain signal is detected in regions where the high affinity α3 Na,K-ATPase isoform but not the α2 Na,K-ATPase is expressed (Fig. 7*G*).

Likewise, in cross-sectional views of fixed, transverse sections of skeletal muscle (Fig. 8), the Na,K-ATPase is detected at every location where BTX, a specific marker of nAChRs on the post-synaptic membrane, is present. In these regions, the α2 antibody and BTX perfectly co-localize. At the NMJ, the α2 Na,K-ATPase label is broader than the BTX label; it is also detected on extrajunctional sarcolemma and in the transverse tubule system, as expected. Together, these results indicate that the nAChR and the Na,K-ATPase α2 isozyme co-localize at the post-synaptic neuromuscular junction.

The Na,K-ATPase α Subunits, the nAChR, and Caveolin-3 Co-immunoprecipitate—The finding that the nAChR co-localizes with the Na,K-ATPase α2 isoform at the NMJ suggests that they may interact via protein-protein associations as part of a membrane complex. To examine this possibility, we measured the ability of the Na,K-ATPase α1 and α2 subunits, the nAChR, and caveolin-3 to co-immunoprecipitate. Caveolin-3 is a muscle-specific member of the caveolin family, which functions as a coordinating center for a variety of signal transduction complexes (35–38). In skeletal muscle, caveolin-3 localization closely parallels that of the Na,K-ATPase α2 isozyme. It is enhanced at the NMJ where it shows a spatial relationship to the nAChR closely similar to that demonstrated here for the Na,K-ATPase α2 isoform (39), and it is present in the transverse tubules (40) and caveolae (41, 42). Caveolin-3 is known to interact directly with several signaling molecules in mature muscle (43, 44) and with the Na,K-ATPase α1 and β1 subunits in cardiac myocytes (45, 46). Here, we show that the Na,K-ATPase α1 (Fig. 9, *left panel*) and Na,K-ATPase α2 (Fig. 9, *middle panel*) subunits each co-immunoprecipitate with the muscle nAChR and caveolin-3. Conversely, the nAChR co-immunoprecipitates with the Na,K-ATPase α1 and α2 subunits (Fig. 9, *right panel*) and with phospholemman (also termed FXYD1), a protein partner of the Na,K-ATPase that is abundant in skeletal muscle. The association between the nAChR, the Na,K-ATPase α subunits, and phospholemman is highly specific. Neither the Na,K-ATPase α subunits (*left* and *middle panels*) nor the nAChR (*right panel*) co-precipitate with sarcoplasmic reticular proteins SERCA2 or phospholamban, which are also present in the muscle lysate. Moreover, no signal was obtained with non-immune serum or beads only, for any protein tested. Finally, no signal was obtained with antibody against GADPH, plasma membrane Ca-ATPase, GLUT4, and GLUT1 (this study).[3]

[3] J. A. Heiny, V. V. Kravtsova, F. Mandel, T. L. Radzyukevich, B. Benziane, A. V. Prokofiev, S. E. Pedersen, A. V. Chibalin, and I. I. Krivoi, unpublished observations.

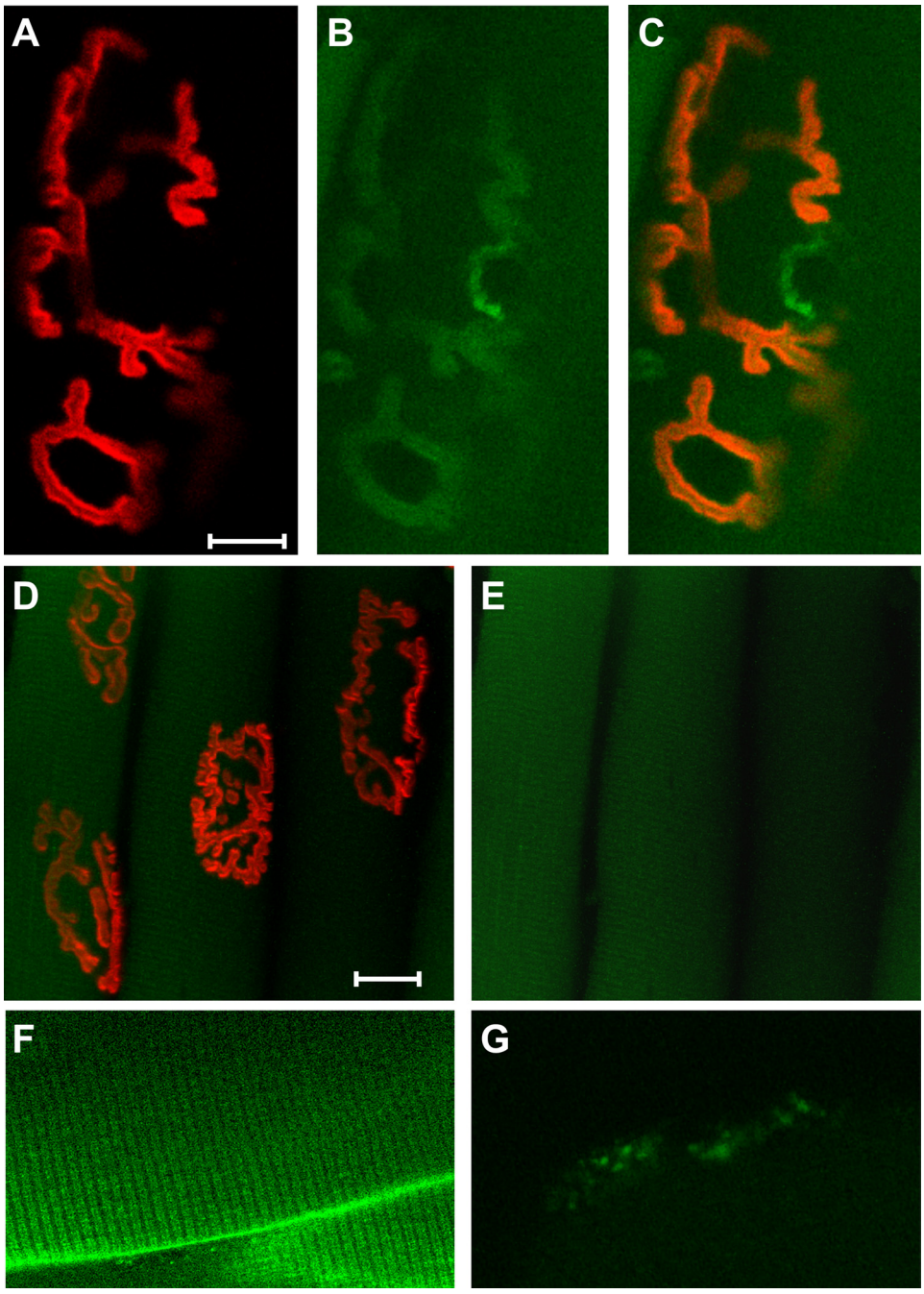

FIGURE 7. **The α2 Na,K-ATPase and nAChR co-localize at the muscle end plate.** *Top row*, longitudinal optical section of a single end plate on a mouse extensor digitorum longus muscle double labeled with rhodamine-conjugated bungarotoxin (0.6 μM) and BODIPY-conjugated ouabain (1 μM). *A*, rhodamine channel, *red*; *B*, BODIPY channel, *green*; and *C*, overlap, *orange*. *Scale bar*, 10 μm. *Middle row*, negative control. End plates from the EDL muscle of a mouse having a ouabain-resistant Na,K-ATPase α2 isoform ($\alpha2^{R/R;}$ (10) do not label with BODIPY-ouabain. *D*, rhodamine and green channels show BTX signal only; *E*, same section as *D* showing BODIPY channel only at ×2 intensity to confirm the absence of BODIPY label at end plates. *Scale bar*, 20 μm. *Bottom row*, positive controls. BODIPY-conjugated ouabain labels the Na,K-ATPase α2 and α3 isoforms in the expected submembrane domains. *F*, BODIPY-ouabain (1 μM) labels the transverse tubules and sarcolemma where the Na,K-ATPase α2 isoform is known to be expressed (51). Note: *double rows* of label with a repeat pattern of two per sarcomere, as expected from the dual transverse-tubule openings at the *A-I* junctions of mammalian muscle. *G*, BODIPY-ouabain (0.5 μM) labels afferent nerve endings at a muscle spindle that express the α3 isoform (68). A freshly isolated muscle from either a wild-type or $\alpha2^{R/R}$ mouse was incubated in physiological buffer containing the conjugated ligands, washed, and imaged using a Zeiss 510 confocal microscope with identical settings on all channels. Control experiments using singly labeled muscles and overlapping emission spectra confirmed that the BODIPY signal is not due to spillover from the rhodamine label. Additional controls confirmed that the BODIPY signal was absent from muscles incubated with excess unlabeled ouabain (1 mM), confirming its specific binding to the Na,K-ATPase (this study).[3] The muscle spindle was identified visually and the presence of α Na,K-ATPase was independently confirmed using anthroyl-ouabain.

Together, these data demonstrate a selective association between the nAChR, the Na,K-ATPase α subunits, phospholemman, and caveolin-3 on the muscle sarcolemma. They support the idea that the nAChR, the Na,K-ATPase, and caveolin-3 associate in skeletal muscle in a protein complex, perhaps with additional protein partners.

Ouabain Binding to the Na,K-ATPase Alters Desensitized States of the nAChR in an Isolated Membrane Preparation—The tight co-localization and specific co-immunoprecipitation of the nAChR with Na,K-ATPase suggests that they may signal through protein-protein interactions. This suggestion is strengthened by our previous finding that nAChR and Na,K-ATPase are able to interact in a highly purified membrane preparation of electrocytes from *T. californica* (1). The electrocyte is a modified muscle cell rich in NMJs, and has been extensively studied as a model for understanding the mammalian synapse and the NMJ. Isolated membrane preparations from this tissue are enriched in nAChRs and Na,K-ATPase. Using this preparation in combination with a fluorescent nicotinic agonist, DC6C, it is possible to follow fast conformational transitions of the nAChR (21, 22) as it transits to the stably desensitized state. DC6C fluorescence is excited by energy transfer from a tryptophan residue near the ACh binding site, and the fluorescence change upon DC6C binding reports conformational transitions of the nAChR to the desensitized state. These transitions occur in at least three phases (21). A fast fluorescence change at 25–50 ms reflects agonist binding to the small population of receptors that already exist in the desensitized state ("predesensitized" nAChRs), and also includes a smaller component of binding to the α-δ site in its resting state (47). This component is followed by intermediate (<1 s) and slow steps of desensitization, reflecting intermediate transitions of the nAChR as it desensitizes. The intermediate

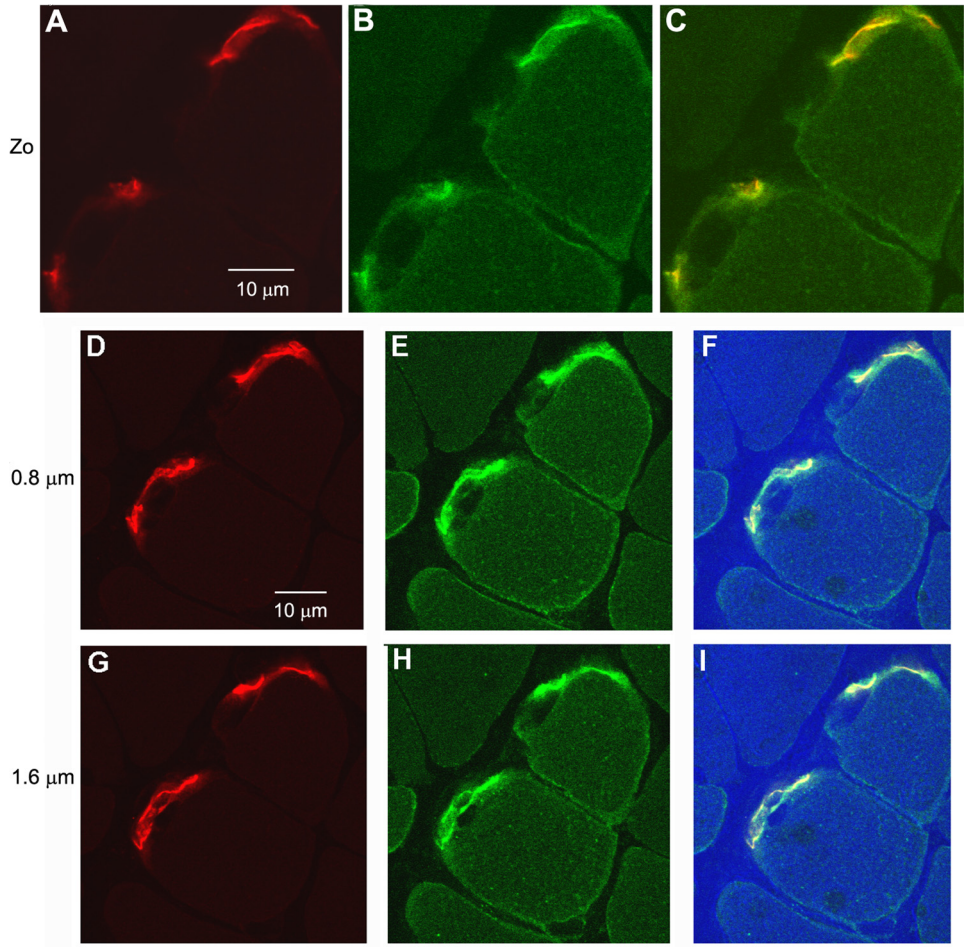

FIGURE 8. **Higher magnification transverse views of fixed skeletal muscle fibers dual labeled with BTX and an Na,K-ATPase α2 isoform-specific antibody.** *A*, BTX (*red*) labels the post-synaptic NMJ of two fibers; *B*, Na,K-ATPase α2 antibody (*green*); *C*, merged image showing overlap of BTX and α2 Na,K-ATPase (*yellow*) at the postsynaptic NMJ. Serial optical sections (*Z* stack) were taken at 0.4-μm intervals through a fixed, transverse section of mouse EDL muscle using a ×100, 1.45 NA oil objective (see "Experimental Procedures" for details). *Panels D–F* and *G–I* show the same region imaged 0.8 and 1.6 μm deeper. *Panels F* and *I* include the transmitted light image (*blue*) to enhance the fiber edges and interstitial regions. The complete *Z* stack is available as "supplemental information".

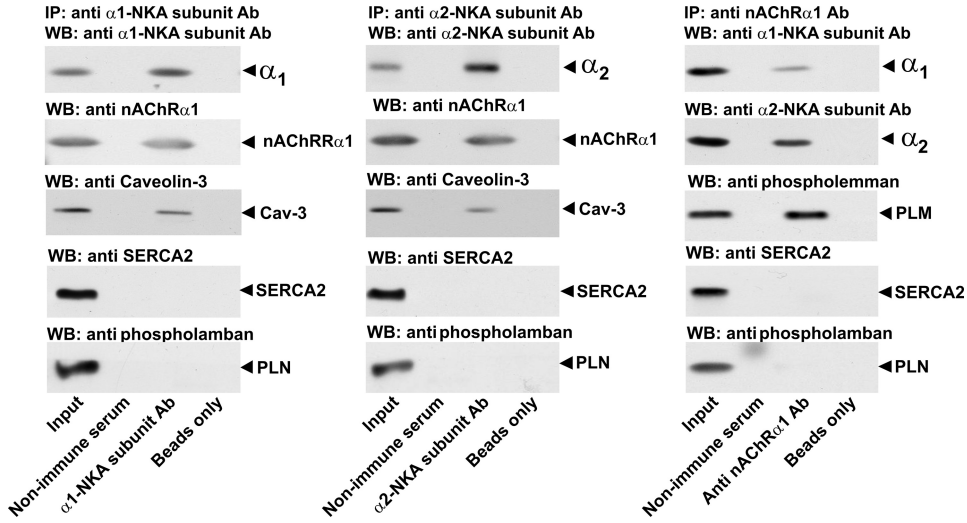

FIGURE 9. **Co-immunoprecipitation of the Na,K-ATPase α1 and α2 subunits with the nAChR and caveolin-3.** Muscle lysates were immunoprecipitated (*IP*) with monoclonal antibodies against the α1 (*left panel*) or α2 subunit (*middle panel*) of the Na,K-ATPase or nAChR (*right panel*), and then probed by Western blot (*WB*) with antibodies against α1 and α2 subunits of Na,K-ATPase, caveolin-3, nAChR, SERCA2, phospholamban (*PLN*), or phospholemman (*PLM*), as indicated. A positive control (*lane 1*, input) confirmed the presence of all species in the muscle lysate prior to immunoprecipitation. Each panel is a representative Western blot from five independent experiments.

transitions may reflect conformations in which the two ligand sites coexist in distinct resting and desensitized states (21, 24, 26, 48). The mixed state intermediate conformations bind DC6C with high affinity (K_d 3–10 nM) (21). A final, slow phase occurs over seconds to minutes as the nAChR transits to the fully desensitized state.

Here, we used the *Torpedo* membrane preparation to determine which nAChR transition is altered when ouabain is bound to the Na,K-ATPase. We followed transitions of the nAChR to the desensitized state under two conditions (Fig. 10): when the Na,K-ATPase is in either a ouabain bound or an unliganded conformation. Ouabain binding stabilizes the Na,K-ATPase in the *E*2-P conformation of its catalytic cycle, a conformation that has been shown to mediate interactions with other signaling molecules (49). In control conditions, DC6C (1 μM) induces the expected conformational changes initiated by agonist binding, *i.e.* a rapid change (25–50 ms), which reports binding to pre-desensitized nAChRs, a transition to intermediate, desensitized states with a time constant near 1 s, and a slower transition to the stably desensitized state. When the same measurement is obtained from membranes pre-equilibrated with 10 or 20 nM ouabain, the intermediate phase is enhanced in an ouabain concentration-dependent manner (Fig. 10*C* and Table 1). There is no change in the most rapid (Fig. 10*B*) or in the slow transition (Fig. 10*D*). In other words, when the Na,K-ATPase is in its ouabain-bound conformation, it is able to enhance formation of an intermediate, desensitized conformation of the nAChR. These findings support our hypothesis that a desensitized conformation of the nAChR interacts with the Na,K-ATPase.

The specificity of this effect on nAChR desensitization is underscored by several findings. It is elicited by nanomolar ouabain concentrations in the range of the K_d for ouabain binding to the *Torpedo*

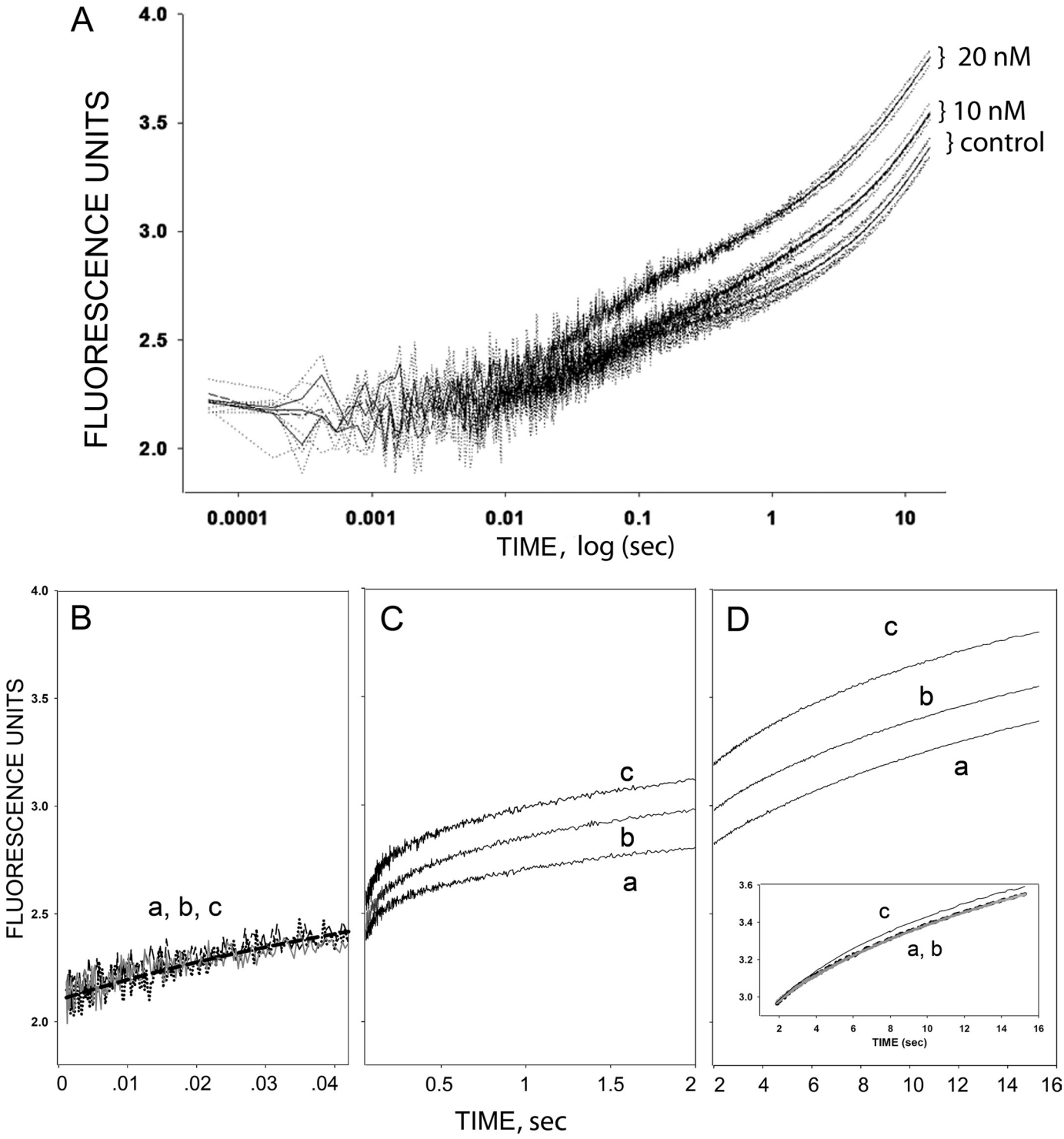

FIGURE 10. **The effect of ouabain on the binding of nAChR agonist to the nAChR in a highly purified membrane fraction from the electric organ of *T. californica*.** The kinetics of DC6C association with the nAChR were followed by monitoring the fluorescent energy transfer from the ACh binding site to a fluorescent agonist, DC6C, as described under "Experimental Procedures." Binding was initiated in a stopped-flow apparatus with rapid mixing. Traces show increases in fluorescence intensity after rapid mixing of a suspension of nAChR-and Na,K-ATPase-rich membrane fragments with 1 μM DC6C in control (*a*), or after a 1-h incubation in 10 nM ouabain (*b*) or 20 nM ouabain (*c*). Each *curve* is the average of 10–20 individual traces, and 3–4 trials performed on the same day are shown for each condition (0, 10, and 20 nM ouabain). Experiments performed on other days yielded similar results with a noticeable difference between the 0 and 10 and 20 nM curves. *Panel A*, the time studied was from 0.1 ms to 15 s. *Panels B-D,* same data with the three phases are plotted on an expanded, linear time scale to better illustrate the distinct kinetic phases of binding. *Panel B* shows the initial 40 ms of binding. The *solid line* is the best single exponential fit to all the rapid binding data ($n = 9 - 12$ trials for each condition). The intermediate binding (0.04–2.0 s) is displayed in *panel C*. *Panel D* covers the time range (2.0–15.0 s) where the slowest binding occurs. The *inset* shows the curves in *Panel D* normalized to their values at 2 s. Labels indicate ouabain concentrations.

TABLE 1

Effect of ouabain on the amplitudes and rate constants of the intermediate desensitized transition (time range 0.025 to 1.0 s, Fig. 10*C*) induced by DC6C binding to the nAChR of *T. californica* (*n* = number of experiments)

[Ouabain]	Amplitudes (*A*)	Rate constants (*k*)
nM	*arbitrary units*	s^{-1}
0 ($n = 4$)	0.21 ± 0.01	2.16 ± 0.17
10 ($n = 3$)	0.32 ± 0.01[a]	1.65 ± 0.08[a]
20 ($n = 3$)	0.29 ± 0.01[a]	1.76 ± 0.12[a]

[a] Significantly different from control at $p < 0.05$.

Na,K-ATPase[3] and it selectively alters a single kinetic transition of the nAChR. In addition, carbamylcholine completely blocks DC6C binding both in the absence and presence of ouabain (this study and see Ref. 1),[3] thereby excluding possible nonspecific effects of ouabain. In addition, the amplitude of the initial rapid phase, which reflects the initial equilibrium between predesensitized and resting states (47), is unaltered. Thus, ouabain does not alter the intrinsic equilibrium between resting and desensitized states in the absence of nicotinic agonist.

DISCUSSION

It has been known for some time that nanomolar concentrations of ACh and other nicotinic agonists produce membrane hyperpolarization in skeletal muscle through a mechanism that involves the nAChR and Na,K-ATPase (1–4). The present study further investigated the molecular mechanisms and membrane localization of this interaction.

Our results show that 1) the interaction between the nAChR and the Na,K-ATPase does not require current flow through open nAChRs; 2) it can be induced in the absence of nicotinic agonists by stabilizing the nAChR in a desensitized state; 3) it operates on both junctional and non-junctional sarcolemma; 4) the nAChR and Na,K-ATPase α2 isoform co-localize at the postsynaptic NMJ; 5) the nAChR co-immunoprecipitates with the Na,K-ATPase α isoforms, phospholemman, and caveolin-3; and 6) in a purified membrane preparation enriched in nAChRs and the Na,K-ATPase, a ouabain-induced conformational change on the Na,K-ATPase can enhance a conformational transition of the nAChR to a desensitized state.

Collectively, these results suggest a mechanism by which the nAChR in a non-conducting, desensitized state, with high apparent affinity for agonist, interacts with the Na,K-ATPase to stimulate active transport. The interaction utilizes a membrane-delimited complex that includes, at a minimum, the nAChR, the Na,K-ATPase α2 isozyme, and caveolin-3. The enhanced electrogenic transport generates a negative potential and membrane hyperpolarization.

Identification of the nAChR Conformation Which Interacts with the Na,K-ATPase—The finding that stimulation of Na,K-ATPase activity by the nAChR in intact muscle does not require current flow or open nAChRs excludes an ionic mechanism for the ACh-induced hyperpolarization. It suggests that a non-conducting, desensitized state of the nAChR may interact with the Na,K-ATPase. Desensitized conformations of the nAChR (stably desensitized as well as intermediate mixed state desensitized transitions) show high apparent affinity for agonist, consistent with the nanomolar agonist concentration dependence of the hyperpolarization. The involvement of a desensitized conformation of the nAChR is further supported by the new findings that: 1) desensitized nAChRs are able to stimulate Na,K-ATPase electrogenic activity, irrespective of whether the nAChR becomes desensitized by prolonged exposure to low, nanomolar concentrations of ACh (the physiological pathway), or by ligands that shift the equilibrium distribution of nAChRs to the desensitized conformation in the absence of agonist binding; 2) the functional interaction of nAChRs with the Na,K-ATPase saturates when the nAChR is maximally desensitized; saturation is not expected from an ionic mechanism except at maximal channel opening, and not with the very low open probability at nanomolar agonist concentrations; and 3) the Na,K-ATPase can interact with a desensitized state of the nAChR in an isolated, highly purified membrane preparation enriched in nAChRs and Na,K-ATPase.

Desensitization is an intrinsic property of the nAChR but its physiological significance is not completely understood (50). One of its roles is to protect against excitotoxicity during repetitive electrical activity by accumulating receptors in a non-conducting conformation. Our findings add regulation of Na,K-ATPase activity, and thereby membrane excitability, to the physiological roles of the desensitized nAChR.

Nature of the Interaction between the nAChR and the Na,K-ATPase—Our findings that the nAChR and Na,K-ATPase co-localize at the postsynaptic NMJ, and that each co-immunoprecipitates with the other and with caveolin-3 suggest that the nAChR and Na,K-ATPase associate as part of a larger protein complex. This suggestion is strengthened by the finding that the nAChR and Na,K-ATPase interact in a highly purified membrane preparation enriched in nAChRs and the Na,K-ATPase and devoid of cytosolic constituents. Together, these findings suggest that the nAChR and Na,K-ATPase interact through membrane-delimited protein-protein interactions, either directly or through additional protein partners.

The physiological significance of the finding that the nAChR also co-immunoprecipitates with the Na,K-ATPase α1 isoform is not known. The α1 isoform is present at the NMJ and surface sarcolemma. However, it does not mediate the hyperpolarization induced by acute exposure to nanomolar ACh or nicotine (1, 2, 4) which, as shown, uses the α2 Na,K-ATPase as the effector target.

Membrane Localization—Our imaging studies demonstrate that the nAChR and Na,K-ATPase α2 isozyme are enhanced and colocalize at the postsynaptic NMJ. The distribution of Na,K-ATPase α2 at the NMJ is broader than that of nAChRs. This spatial relationship at the NMJ is identical to that previously shown between the nAChR and caveolin-3 at the NMJ (39). It is also consistent with the findings that the nAChR, Na,K-ATPase α2, and caveolin-3 co-immunoprecipitate, and that the nAChR interacts with only a subset of the Na,K-ATPase α2 pool in muscle (1).

It was not possible to use imaging to search for colocalization on other membrane regions due to the low density of extrajunctional nAChRs. However, our functional measurements indicate that ACh-induced hyperpolarization also operates on extrajunctional sarcolemma. The submembrane localization of extrajunctional nAChRs in skeletal muscle is not known. It is possible that this interaction occurs in caveolae where the

Na,K-ATPase α2 and caveolin-3 co-localize (42, 51). The possibility that the nAChR and Na,K-ATPase α2 may also interact in the transverse tubules cannot be excluded. The Na,K-ATPase α2 isoform is abundant in the transverse tubules; however, caveolin-3 expression is low in the transverse tubules of mature muscle (52, 53) and the nAChR is present only in trace amounts (54).

The nAChR and Na,K-ATPase as Signalosomes—The Na,K-ATPase forms signaling complexes with a number of membrane-associated proteins; in cardiac and other cells, including the sodium calcium exchanger, epidermal growth factor receptor, Src, and other partners. These signalosomes regulate transmembrane calcium flux, contractility, and cell growth (46, 55–57). The Na,K-ATPase can also interact with neuronal dopamine receptors in a regulatory complex with reciprocal regulation of function (58), and with the glutamate transporter (59). Likewise, the nAChR interacts with multiple signaling partners in a macromolecular complex. Similar to other neurotransmitter receptor complexes, the nAChR is linked via adaptor proteins that also link the receptors to signaling enzymes, adaptor and scaffolding proteins, kinases, and transcription factors. Proteins of the postsynaptic NMJ include the muscle-specific kinase MuSK interacting with MASC; the tyrosine kinases neuregulin and epidermal growth factor receptor; rapsyn, plectin, β-dystroglycan, caveolin-3; and other signaling and transcription factors (60–61). A subset of these proteins are also present in muscle caveolae. Interestingly, chronic stimulation of the nAChR increases expression of the Na,K-ATPase α2 (but not α1) subunit (62). Our results indicate that the Na,K-ATPase α2 subunit is a protein signaling partner with the nAChR at the mammalian NMJ.

Physiological Roles of the Na,K-ATPase α2 Isoform—The Na,K-ATPase α2 isoform is the major expressed isoform of adult skeletal muscle, and comprises 60–87% of total α content (63, 64). Despite its greater abundance, electrogenic transport by the α2 isozyme contributes only approximately -4 mV to the resting potential, compared with -14 mV generated by α1 transport activity (1, 2). This indicates that the α2 isozyme is significantly less active in resting muscle than expected from its abundance. A similar conclusion was reached using muscles of mice with reduced α2 expression (65). These and findings from other laboratories have led to the proposal that the Na,K-ATPase α2 may be the more regulated isoform that can be stimulated under conditions of increased demand. Consistent with this idea, the Na,K-ATPase α2 isoform and its cardiac glycoside binding site participate in the rapid stimulation of Na,K-ATPase transport that occurs during muscle contraction (66). This study adds nAChR-mediated stimulation of electrogenic transport to the mechanisms that can modulate Na,K-ATPase α2 activity.

Physiological Significance of the Interaction Between the nAChR and the Na,K-ATPase α2—Electrogenic transport by the Na,K-ATPase makes an important contribution to the resting membrane potential of skeletal muscle, generating -15 to -20 mV compared with only a few millivolts in other tissues. This large electrogenic potential helps keep the muscle resting potential at its characteristic negative value (-80 to -90 mV) compared with nerve (-70 mV) and maintains the muscle in a responsive state to nerve input. An increase in the electrogenic component of the resting potential is expected to have significant consequences on membrane excitability because it operates over the same voltage range as sodium channel slow inactivation. Slow inactivation is steeply voltage-dependent near the resting potential, changing approximately 3-fold per 6 mV (8, 9). A relatively small hyperpolarization in this voltage range redistributes sodium channels from the inactive to available state. Sodium channels are concentrated near nAChRs at the postsynaptic NMJ where their density is 20-fold that of extrajunctional sarcolemma (32). This clustering insures efficient neuromuscular transmission (67). Consequently, a small hyperpolarization can modulate the responsiveness of the muscle to nerve input, and greatly enhance the effectiveness of synaptic transmission. Moreover, because this mechanism also operates on extrajunctional regions, the excitability of the entire muscle sarcolemma is matched to the enhanced responsiveness of the NMJ. This provides maximally effective excitation of the entire muscle fiber.

Extracellular concentrations of ACh arising from non-quantal release ($\leq$50 nM) are normally present at the NMJ and induce the small, surplus hyperpolarization that is regularly observed near the end plates of resting skeletal muscles (6, 7). Also, nanomolar concentrations of ACh remain in the junctional and muscle interstitial spaces for some time following nerve activity. These low levels may maintain the effectiveness of neuromuscular transmission and "prime" the muscle to respond to an increased level of nerve activity. Overall, an interaction by which ACh acting on the nAChR can regulate the transport activity of the Na,K-ATPase α2 enzyme, and thereby the resting potential, in the voltage range of sodium channel slow inactivation is expected to provide a sensitive mechanism to match membrane excitability to muscle use.

Acknowledgments—We thank Dr. Marshall Montrose and the Live Microscopy Core of the University of Cincinnati for expert assistance, and Drs. Jerry Lingrel and Dr. Nicholas ("Spike") Sperelakis for comments on the manuscript. We thank Dr. Jerry Lingrel for providing the $\alpha 2^{R/R}$ mice.

REFERENCES

1. Krivoi, I. I., Drabkina, T. M., Kravtsova, V. V., Vasiliev, A. N., Eaton, M. J., Skatchkov, S. N., and Mandel, F. (2006) *Pflugers Arch.* **452,** 756–765
2. Krivoi, I., Vasiliev, A., Kravtsova, V., Dobretsov, M., and Mandel, F. (2003) *Ann. N.Y. Acad. Sci.* **986,** 639–641
3. Krivoĭ, I. I., Drabkina, T. M., Dobretsov, M. G., Vasil'ev, A. N., Kravtsova, V. V., Eaton, M. J., Skachkov, S. N., and Mandel, F. (2004) *Ross. Fiziol. Zh. Im. I. M. Sechenova.* **90,** 59–72
4. Kravtsova, V. V., Drabkina, T. M., Prokof'ev, A. V., Kubasov, I. V., Vasil'ev, A. N., and Krivoĭ, I. I. (2008) *Ross. Fiziol. Zh. Im. I. M. Sechenova.* **94,** 1181–1190
5. Akk, G., and Auerbach, A. (1999) *Br. J. Pharmacol.* **128,** 1467–1476
6. Vyskocil, F., Nikolsky, E., and Edwards, C. (1983) *Neuroscience* **9,** 429–435
7. Nikolsky, E. E., Zemková, H., Voronin, V. A., and Vyskocil, F. (1994) *J. Physiol.* **477,** 497–502
8. Ruff, R. L., Simoncini, L., and Stühmer, W. (1987) *J. Physiol.* **383,** 339–348
9. Ruff, R. L., Simoncini, L., and Stühmer, W. (1988) *Muscle Nerve* **11,** 502–510
10. Dostanic, I., Lorenz, J. N., Schultz, J. J., Grupp, I. L., Neumann, J. C., Wani,

M. A., and Lingrel, J. B. (2003) *J. Biol. Chem.* **278,** 53026–53034
11. Henning, R. H., Nelemans, S. A., van den Akker, J., and den Hertog, A. (1994) *Br. J. Pharmacol.* **111,** 459–464
12. Hicks, A., and McComas, A. J. (1989) *J. Physiol.* **414,** 337–349
13. Carlson, C. G., and Roshek, D. M. (2001) *Pflugers Arch.* **442,** 369–375
14. Sperelakis, N. (2001) in *Cell Physiology Sourcebook*, 3rd Ed., pp. 231–236 Academic Press, New York
15. Everts, M. E., and Clausen, T. (1994) *Am. J. Physiol. Cell Physiol.* **266,** C925–934
16. Pressley, T. A. (1992) *Am. J. Physiol. Cell Physiol.* **262,** C743–751
17. Pritchard, T. J., Parvatiyar, M., Bullard, D. P., Lynch, R. M., Lorenz, J. N., and Paul, R. J. (2007) *Am. J. Physiol. Heart Circ. Physiol.* **293,** H1172–1182
18. Pedersen, S. E., Dreyer, E. B., and Cohen, J. B. (1986) *J. Biol. Chem.* **261,** 13735–13743
19. Kawakami, K., Noguchi, S., Noda, M., Takahashi, H., Ohta, T., Kawamura, M., Nojima, H., Nagano, K., Hirose, T., and Inayama, S. (1985) *Nature* **316,** 733–736
20. Waksman, G., Fournié-Zaluski, M. C., and Roques, B. (1976) *FEBS Lett.* **67,** 335–342
21. Song, X. Z., Andreeva, I. E., and Pedersen, S. E. (2003) *Biochemistry* **42,** 4197–4207
22. Raines, D. E., and Krishnan, N. S. (1998) *Biochemistry* **37,** 956–964
23. Spitzmaul, G., Gumilar, F., Dilger, J. P., and Bouzat, C. (2009) *Br. J. Pharmacol.* **157,** 804–817
24. Ryan, S. E., Blanton, M. P., and Baenziger, J. E. (2001) *J. Biol. Chem.* **276,** 4796–4803
25. Song, X. Z., and Pedersen, S. E. (2000) *Biophys. J.* **78,** 1324–1334
26. Prince, R. J., and Sine, S. M. (1999) *J. Biol. Chem.* **274,** 19623–19629
27. Wilson, G., and Karlin, A. (2001) *Proc. Natl. Acad. Sci. U.S.A.* **98,** 1241–1248
28. Auerbach, A., and Akk, G. (1998) *J. Gen. Physiol.* **112,** 181–197
29. Mourot, A., Rodrigo, J., Kotzyba-Hibert, F., Bertrand, S., Bertrand, D., and Goeldner, M. (2006) *Mol. Pharmacol.* **69,** 452–461
30. Gentry, C. L., and Lukas, R. J. (2001) *J. Pharmacol. Exp. Ther.* **299,** 1038–1048
31. Boyd, N. D., and Cohen, J. B. (1984) *Biochemistry* **23,** 4023–4033
32. Caldwell, J. H. (2000) *Microsc. Res. Tech.* **49,** 84–89
33. Sweadner, K. J. (1989) *Biochim. Biophys. Acta* **988,** 185–220
34. Zahler, R., Sun, W., Ardito, T., Zhang, Z. T., Kocsis, J. D., and Kashgarian, M. (1996) *Circ. Res.* **78,** 870–879
35. Harder, T., and Simons, K. (1997) *Curr. Opin. Cell Biol.* **9,** 534–542
36. Isshiki, M., and Anderson, R. G. (1999) *Cell Calcium* **26,** 201–208
37. Galbiati, F., Razani, B., and Lisanti, M. P. (2001) *Trends Mol. Med.* **7,** 435–441
38. Galbiati, F., Razani, B., and Lisanti, M. P. (2001) *Cell* **106,** 403–411
39. Carlson, B. M., Carlson, J. A., Dedkov, E. I., and McLennan, I. S. (2003) *J. Histochem. Cytochem.* **51,** 1113–1118
40. Ralston, E., and Ploug, T. (1999) *Exp. Cell Res.* **246,** 510–515
41. Voldstedlund, M., Vinten, J., and Tranum-Jensen, J. (2001) *Cell Tissue Res.* **306,** 265–276
42. Ockleford, C. D., Cairns, H., Rowe, A. J., Byrne, S., Scott, J. J., and Willingale, R. (2002) *J. Microsc.* **206,** 93–105
43. García-Cardeña, G., Martasek, P., Masters, B. S., Skidd, P. M., Couet, J., Li, S., Lisanti, M. P., and Sessa, W. C. (1997) *J. Biol. Chem.* **272,** 25437–25440
44. Sunada, Y., Ohi, H., Hase, A., Ohi, H., Hosono, T., Arata, S., Higuchi, S., Matsumura, K., and Shimizu, T. (2001) *Hum. Mol. Genet.* **10,** 173–178
45. White, C. N., Figtree, G. A., Liu, C. C., Garcia, A., Hamilton, E. J., Chia, K. K., and Rasmussen, H. H. (2009) *Am. J. Physiol. Cell Physiol.* **296,** C693–C700
46. Liu, L., and Askari, A. (2006) *Am. J. Physiol. Cell Physiol.* **291,** C569–578
47. Andreeva, I. E., Nirthanan, S., Cohen, J. B., and Pedersen, S. E. (2006) *Biochemistry* **45,** 195–204
48. Prince, R. J., and Sine, S. M. (1998) *J. Biol. Chem.* **273,** 7843–7849
49. Li, Z., and Xie, Z. (2009) *Pflugers Arch.* **457,** 635–644
50. Giniatullin, R., Nistri, A., and Yakel, J. L. (2005) *Trends Neurosci.* **28,** 371–378
51. Williams, M. W., Resneck, W. G., Kaysser, T., Ursitti, J. A., Birkenmeier, C. S., Barker, J. E., and Bloch, R. J. (2001) *J. Cell Sci.* **114,** 751–762
52. Rahkila, P., Takala, T. E., Parton, R. G., and Metsikkö, K. (2001) *Exp. Cell Res.* **267,** 61–72
53. Parton, R. G., Way, M., Zorzi, N., and Stang, E. (1997) *J. Cell Biol.* **136,** 137–154
54. Jaimovich, E., Donoso, P., Liberona, J. L., and Hidalgo, C. (1986) *Biochim. Biophys. Acta* **855,** 89–98
55. Pierre, S. V., and Xie, Z. (2006) *Cell Biochem. Biophys.* **46,** 303–316
56. Blaustein, M. P., Zhang, J., Chen, L., Song, H., Raina, H., Kinsey, S. P., Izuka, M., Iwamoto, T., Kotlikoff, M. I., Lingrel, J. B., Philipson, K. D., Wier, W. G., and Hamlyn, J. M. (2009) *Hypertension* **53,** 291–298
57. Xie, Z., and Askari, A. (2002) *Eur. J. Biochem.* **269,** 2434–2439
58. Hazelwood, L. A., Free, R. B., Cabrera, D. M., Skinbjerg, M., and Sibley, D. R. (2008) *J. Biol. Chem.* **283,** 36441–36453
59. Rose, E. M., Koo, J. C., Antflick, J. E., Ahmed, S. M., Angers, S., and Hampson, D. R. (2009) *J. Neurosci.* **29,** 8143–8155
60. Bezakova, G., and Ruegg, M. A. (2003) *Nat. Rev. Mol. Cell Biol.* **4,** 295–308
61. Nazarian, J., Hathout, Y., Vertes, A., and Hoffman, E. P. (2007) *Proteomics* **7,** 617–627
62. Kragenbrink, R., Higham, S. C., Sansom, S. C., and Pressley, T. A. (1996) *Synapse* **23,** 219–223
63. Orlowski, J., and Lingrel, J. B. (1988) *J. Biol. Chem.* **263,** 10436–10442
64. He, S., Shelly, D. A., Moseley, A. E., James, P. F., James, J. H., Paul, R. J., and Lingrel, J. B. (2001) *Am. J. Physiol. Regul. Integr. Comp. Physiol.* **281,** R917–R925
65. Radzyukevich, T. L., Moseley, A. E., Shelly, D. A., Redden, G. A., Behbehani, M. M., Lingrel, J. B., Paul, R. J., and Heiny, J. A. (2004) *Am. J. Physiol. Cell Physiol.* **287,** C1300–C1310
66. Radzyukevich, T. L., Lingrel, J. B., and Heiny, J. A. (2009) *Proc. Natl. Acad. Sci. U.S.A.* **106,** 2565–2570
67. Wood, S. J., and Slater, C. R. (2001) *Prog. Neurobiol.* **64,** 393–429
68. Dobretsov, M., Hastings, S. L., Sims, T. J., Stimers, J. R., and Romanovsky, D. (2003) *Neuroscience* **116,** 1069–1080